

Single Image Texture Translation for Data Augmentation

Boyi Li^{1,2} Yin Cui³ Tsung-Yi Lin³ Serge Belongie^{1,2}

¹Cornell University ²Cornell Tech ³Google Research, Brain Team

Abstract

Recent advances in image synthesis enables one to translate images by learning the mapping between a source domain and a target domain. Existing methods tend to learn the distributions by training a model on a variety of datasets, with results evaluated largely in a subjective manner. Relatively few works in this area, however, study the potential use of semantic image translation methods for image recognition tasks. In this paper, we explore the use of Single Image Texture Translation (SITT) for data augmentation. We first propose a lightweight model for translating texture to images based on a single input of source texture, allowing for fast training and testing. Based on SITT, we then explore the use of augmented data in long-tailed and few-shot image classification tasks. We find the proposed method is capable of translating input data into a target domain, leading to consistent improved image recognition performance. Finally, we examine how SITT and related image translation methods can provide a basis for a data-efficient, augmentation engineering approach to model training.

1. Introduction

“The Forms are not limited to geometry. For any conceivable thing or property there is a corresponding Form, a perfect example of that thing or property. The list is almost inexhaustible.”

—Plato “Theory of Forms”

Recent years have witnessed a breakthrough in deep learning based image synthesis such as image translation [9, 21, 27] that manipulates or synthesizes images using neural networks rather than hand-crafted techniques, such as guided filtering [13] or image quilting [7]. However, few of them study the potential use of semantic image synthesis methods as an effective data augmentation tool for recognition tasks. The progress is mainly limited by two bottlenecks: the validity of synthetic data for target labels and the running time. With regard to data validity, many works such as Stylized-ImageNet [10] propose to apply style transfer to the original dataset for pre-training to improve the model’s robustness, but the synthetic images lack the natural appearance of the original images. Also, since it deconstructs

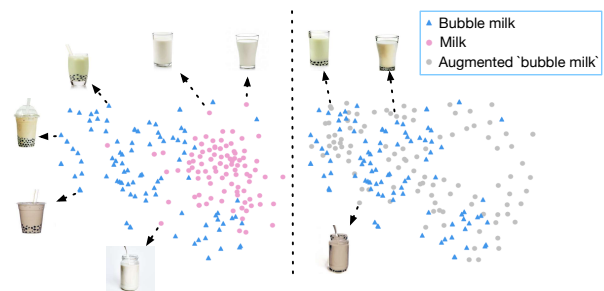


Figure 1. t-SNE embedding before and after applying SITT. Left: milk (red) and bubble milk (blue) images. Right: corresponding augmented ‘bubble milk’ (gray) and original bubble milk images.

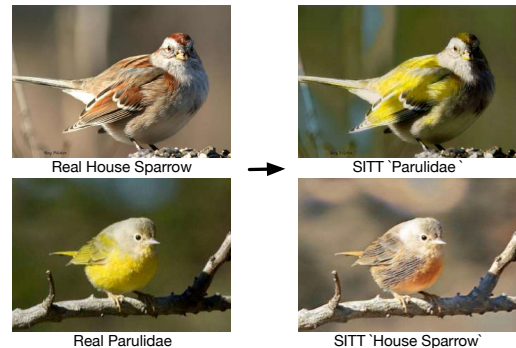


Figure 2. SITT translates the texture from one image to another.

texture and content in the original images, it will hurt the recognition performance if trained with the augmented data, and needs to be fine-tuned using only the original dataset to obtain a benefit. Though many approaches [31, 57, 17] have proposed advanced algorithms to translate style and texture, most of them still focus on a subjective evaluation. With regard to running time, current techniques [35, 24] usually needs to train for at least several hours. This seriously hinders its use for data augmentation in real applications. While in the domain of data augmentation, current methods mainly focus on pixel-level or geometric operations such as blur or crop [36]. The potential of augmenting data into different domains, however, is relatively unexplored.

In light of this, we propose *Single Image Texture Translation* (SITT) for data augmentation. It enables texture translation or swapping trained with a single texture source input. We believe an ideal image synthesis method for data aug-

mentation should yield visually appealing results, improved recognition performance as well as time efficiency. SITT is the first of few methods that explore this problem and try to balance all these factors. Our model is lightweight and permits fast training (< 5 min) and testing (9 ms) on a 288×288 image using a single Geforce GTX 1080 Ti GPU. In Figure 1, we illustrate an example of generated ‘bubble milk’ images by translating the texture of bubble milk to milk images. We visualize the image distribution using t-SNE [26]. We collect 100 natural milk images and 100 natural bubble milk images from the Web, shown on the left. On the right, we can see that the SITT ‘bubble milk’ images align well with the original bubble milk images, which hints the efficacy of SITT for semantic data augmentation. The intuition of replacing texture is conceptually similar to the arithmetic properties of word embeddings [2], e.g., $\overrightarrow{\text{Milk}} - \overrightarrow{\text{texture}(\text{Milk})} + \overrightarrow{\text{texture}(\text{BubbleMilk})} = \overrightarrow{\text{BubbleMilk}}$. In Figure 2, we illustrate another texture swapping example between two species of birds, while preserving the natural appearances. More details could be found at <https://boyiliee.github.io/sitt.github.io>. Code will be available at <https://github.com/Boyiliee/SITT>.

Our key contributions in this work are as follows.

1. A lightweight Single Image Texture Translation (SITT) model that translates textures from a single image to another image.
2. We explore the use of SITT for semantic data augmentation, aiming to augment data towards the target texture domain. As an example, we translate texture from rare diseased leaves to abundant healthy leaves to augment training data and improve model performance in a plant pathology challenge dataset [41].
3. We dig deeper into the use of SITT for augmenting data and demonstrate its effectiveness in several image recognition tasks (e.g., improving the performance of ResNet-18 by 1.4% for 5-shot classification on CUB-200-2011), which sheds light on the potential direction of image synthesis for data augmentation in the wild.

2. Related Work

Image Synthesis. Deep learning based image synthesis manipulates images through the design of various generative neural networks. Fueled by the explorations in generative models such as GAN [11] and VAE [19], researchers have explored ideas such as neural style transfer and image translation. A neural algorithm of artistic style (ArtStyle) [9] can separate and recombine the image content and style of natural images. CycleGAN [57] investigates the use of conditional adversarial networks as a general-purpose solution to image-to-image translation problems. SinGAN [35]

demonstrates success in single image retargeting. Few-Shot Unsupervised Image-to-Image Translation (UNIT) [25] focuses on previously unseen target classes that are specified at test time only by a few example images. TuiGAN [24] aims to learn versatile image-to-image translation with two unpaired images for image-to-image translation designed in a coarse-to-fine manner. Furthermore, [50, 31, 30] propose elegant methods for better preserving their structural information and statistical properties. However, these methods focus more on a subjective manner instead of considering all factors including decent outputs, time efficiency, improved recognition results, as well as flexibility with various input resolutions for data augmentation.

Data Augmentation. Data augmentation plays a critical role in various image recognition tasks [4]. On the one hand, basic image manipulation methods have been widely used as effective pre-processing tools [36, 37, 10, 46, 22, 12, 3], with examples including flipping, rotation, jittering, grayscale, and Gaussian blur. Several works [43, 5] explore effective combined choices of basic image manipulations. LOOC [49] searches for an optimal augmentation strategy among a large pool of candidates based on specific datasets or tasks. Mixup [52] interpolates two training inputs in feature and label space simultaneously. CutMix [51] uses a copy-paste strategy and mixes the labels in proportion to the number of pixels contributed by each input image to the final composition. On the other hand, many researchers have begun to explore the impact of semantic data augmentation for real-world image recognition tasks [53, 37, 46, 1]. Geirhos *et al.* [10] find that CNNs like ResNet-50 favor texture rather than shape, and appropriate use of augmented ImageNet via style transfer could alleviate this bias and improve the model performance. In addition, [56, 39, 55, 33] aim to learn robust shape-based features for domain generalization. RL-CycleGAN [34] introduces a consistency loss for simulation-to-real-world transfer for reinforcement learning. However, few of them explicitly augment data with natural outputs that could be used to solve real problems. In this paper, we propose SITT that generates new data semantically via domain-specific texture translation. We provide a simplified illustration of the data augmentation landscape in Figure 3.

3. Method

3.1. Single Image Texture Translation

Framework. Figure 4 shows a brief sketch of our framework. In the illustrated example, SITT aims to translate texture from a single source texture image (Input B: Parulidae) to a content image (Input A: House Sparrow) and get a synthetic ‘Parulidae’ image. SITT consists of three parts: shared Texture Encoder (En_T), shared Content Encoder (En_C) and corresponding Decoder De_A and De_B for in-

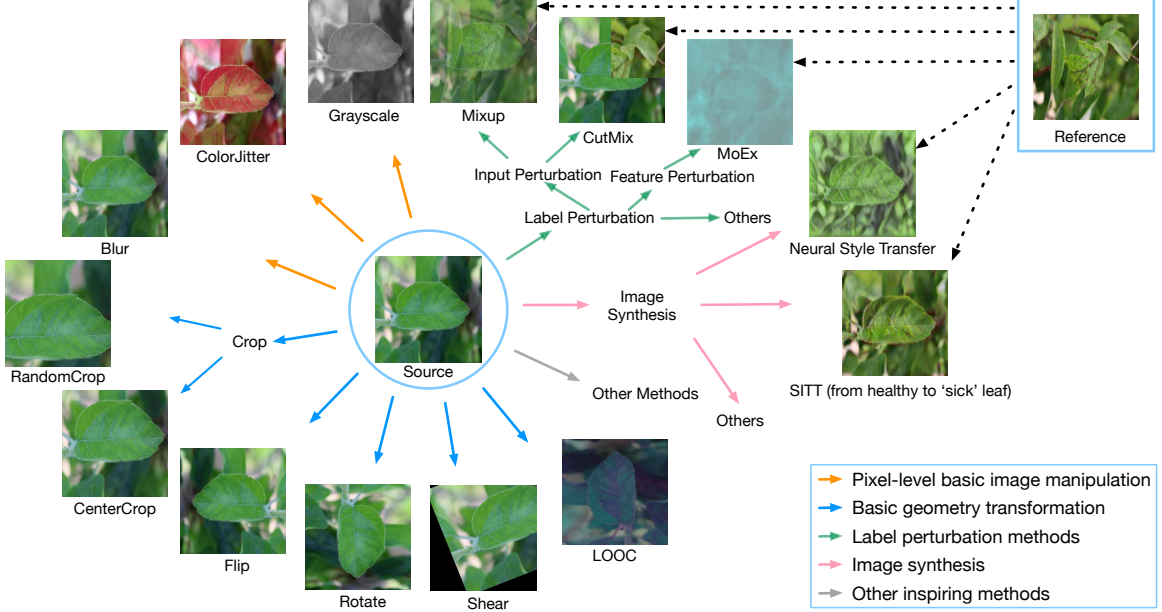


Figure 3. Overview of the data augmentation landscape.

put A and B. We first feed input B into En_T to obtain the texture latent vector and feed input A into En_C to get the content (structure) matrix. Then we concatenate the texture and content features and feed them into Decoder to generate the output image.

Model Design. To efficiently preserve structure and extract textures with an optimal number of layers, we apply two downsampling operations during training. To achieve efficient model design, we emphasize three critical components: input augmentation, structural information re-injection, texture latent regression.

(1) Input augmentation. We propose to directly augment input by Horizontal Flip, CenterCrop, and RandomCrop.¹ We find such input augmentation could effectively guarantee the diversity of image scales for fast and efficient training.

(2) Structural information re-injection. To better preserve the structural information and optimize training, we apply Positional Norm [23] in En_C to extract intermediate normalization constants mean μ and standard deviation σ as structural features β and γ and re-inject them into the later layers of Decoder to transfer structural information. Given the activations $X \in \mathbb{R}^{B \times C \times H \times W}$ (where B denotes the batch size, C the number of channels, H the height, and W the width) in a given layer of a neural net, the extracting

¹For RandomCrop, we crops the given image to a new scale and resizes the crop to the given size. To preserve the structure or texture characteristics, we set the scale $\in (0.8, 1)$.

operations² are listed as:

$$\beta = \mu_{b,h,w} = \frac{1}{C} \sum_{c=1}^C X_{b,c,h,w}, \quad (1)$$

$$\gamma = \sigma_{b,h,w} = \sqrt{\frac{1}{C} \sum_{c=1}^C (X_{b,c,h,w} - \mu_{b,h,w})^2 + \epsilon}. \quad (2)$$

The re-injecting operation after i th intermediate layer is listed as:

$$\text{Out}_i(\mathbf{x}) = \gamma_i F_i(\mathbf{x}) + \beta_i, \quad (3)$$

where the function F is modeled by the intermediate layers. We summarize the SITT workflow in Appendix Section A.

(3) Texture latent regression. To achieve better representation disentanglement [20] for texture and content, we use a latent regression loss L_{idt} to encourage the invertible mapping between the latent texture vectors and the corresponding outputs and enforce the reconstruction based on the latent texture vectors.

Loss Function. SITT is based on GAN framework [11], the loss function is composed of 5 parts: adversarial loss L_{adv} , latent regression loss L_{idt} , content matrix reconstruction loss L_{rec} , texture vector KL divergence loss L_{kl} and perceptual loss L_f . During training, we have inputs I_A and I_B , extracted texture vectors T_A and T_B , content matrix C_A and C_B , corresponding normalization constants β_A, γ_A and β_B, γ_B , as well as outputs I'_A and I'_B .

²The ϵ is a small stability constant (e.g., $\epsilon = 10^{-5}$) to avoid divisions by zero and pixel values due to numerical inaccuracies.

Adversarial loss is GAN standard loss function for matching the distribution of translated image to the target domain:

$$L_{adv} = \mathbb{E}[\log D_B(I_B)] + \mathbb{E}[1 - \log D_B(I'_B))] + \mathbb{E}[\log D_A(I_A)] + \mathbb{E}[1 - \log D_A(I'_A))] \quad (4)$$

we have two discriminators D_A, D_B for distinguishing between real and generated image for A and B domain separately.

L_{idt} makes sure the decoder is able to reconstruct it based on extracted content matrix and texture latent vector:

$$L_{idt} = \mathbb{E}[||I_{BB} - I_B||_1] + \mathbb{E}[||I_{AA} - I_A||_1], \quad (5)$$

where

$$I_{AA} = De_A(T_A, En_C(I_A)), I_{BB} = De_B(T_B, En_C(I_B)).$$

L_{rec} is based on Cycle-Consistency loss [57] that optimizes the training for this under-constrained problem and regularize the translated image to preserve semantic structure of the input image:

$$L_{rec} = \mathbb{E}[||I'_{BA} - I_A||_1] + \mathbb{E}[||I'_{AB} - I_B||_1], \quad (6)$$

where

$$I'_{BA} = De_A(T_A, En_C(I'_B)), I'_{AB} = De_B(T_B, En_C(I'_A)).$$

To better preserve the structural information, we use perceptual loss L_f [18] based on VGG19 [38] between the generated outputs and original Inputs. We use KL divergence loss L_{kl} [16, 20] to minimize the distribution variance between extracted texture vectors from the target image and generated image.

Our final objective function is:

$$L_{all} = L_{adv} + \lambda_{idt}L_{idt} + \lambda_{rec}L_{rec} + \lambda_{kl}L_{kl} + \lambda_fL_f, \quad (7)$$

where $\lambda_{adv}, \lambda_{idt}, \lambda_{rec}, \lambda_{kl}$ and λ_f are weights assigned for each loss, respectively.

3.2. SITT for Data Augmentation

SITT aims to augment images that align with the target texture domain and could be used as extra training data for various recognition tasks. Assume we have plenty of source domain images SetA but a few target domain images SetB, the only difference between SetA and SetB is that they contain different textures. Our goal is to synthesize extra ‘B’ data by replacing textures of SetA with the new textures from SetB, we call the augmented dataset as AugSetB. Based on SITT, we have two ways to achieve this: i) *Single to Single*. Since SITT enables translating textures between two single images, we train and generate new image I'_B based on every input I_A and I_B from SetA and SetB, respectively. ii) *Single to Multi*. We train and generate new image I'_B with a single source texture image I_B from SetB and all content images from SetA. Please see Section B in the Appendix for workflow details.

4. SITT Experiments

4.1. Experimental Setup

During training, we use Adam with 0.0005 learning rate, $\beta_1 = 0.5$ and $\beta_2 = 0.999$. We augment the inputs and resize them to 288×288 . Empirically, we find the model starts to converge after 600 iterations and become stable after 800 iterations for every input pair. We use widely-used dataset [57] as well as images collected from the Internet (including VanillaCake \leftrightarrow ChocolateCake, Milk \leftrightarrow BubbleMilk, etc.). We will release our Pytorch [32] implementation and associated data to facilitate future research.

4.2. Image Translation Results

We refer to the experimental setup of TuiGAN [24] that randomly selects 8 unpaired images, and generate 8 translated images for 4 unpaired image to image translation tasks including Horse \leftrightarrow Zebra, Apple \leftrightarrow Orange, VanillaCake \leftrightarrow ChocolateCake and Milk \leftrightarrow BubbleMilk. We train and test with a single source image and target texture image. We compare our results with various popular or most recent image synthesis methods with their official code and setting: ArtStyle [8], CycleGAN [57], SinGAN [35]³, FUNIT [25] and TuiGAN [24]. For evaluation, we use three of most popular metrics: Fréchet Inception Distance (FID) [15], Learned Perceptual Image Patch Similarity (LPIPS) [54] and VGG Loss (perceptual loss) [18]. FID aims to capture the similarity of generated images to real ones, LPIPS is used to estimate how likely the outputs are to belong to the target domain, VGG Loss (with VGG19) is used to estimate how much the outputs preserve the structural information in the inputs. We randomly select 32 images and run the experiments for 3 times with a single source and target image, we report the average score in Table 1. We could notice that SITT could achieve comparatively better scores. In Fig 5, we show the corresponding qualitative comparison results. We could observe that SITT enables clear and reasonable output and works for various categories such as VanillaCake \leftrightarrow ChocolateCake and Milk \leftrightarrow BubbleMilk. However, for these two tasks, ArtStyle fails to learn the bubble or cake patterns, CycleGAN works better while losing detailed structural or textural information, FUNIT generates unnatural images, SinGAN doesn’t change the textures appropriately and TuiGAN fails to generate reasonable samples based on multiple scales, leading to unreasonable or distorted outputs. Instead, SITT doesn’t depend on multi-scale training, which is more robust for random inputs of different resolutions.

4.3. Ablation Study

Given that SITT aims to learn a texture mapping between source image and target image but preserve general content,

³We first train SinGAN model and apply it to Paint to Image.

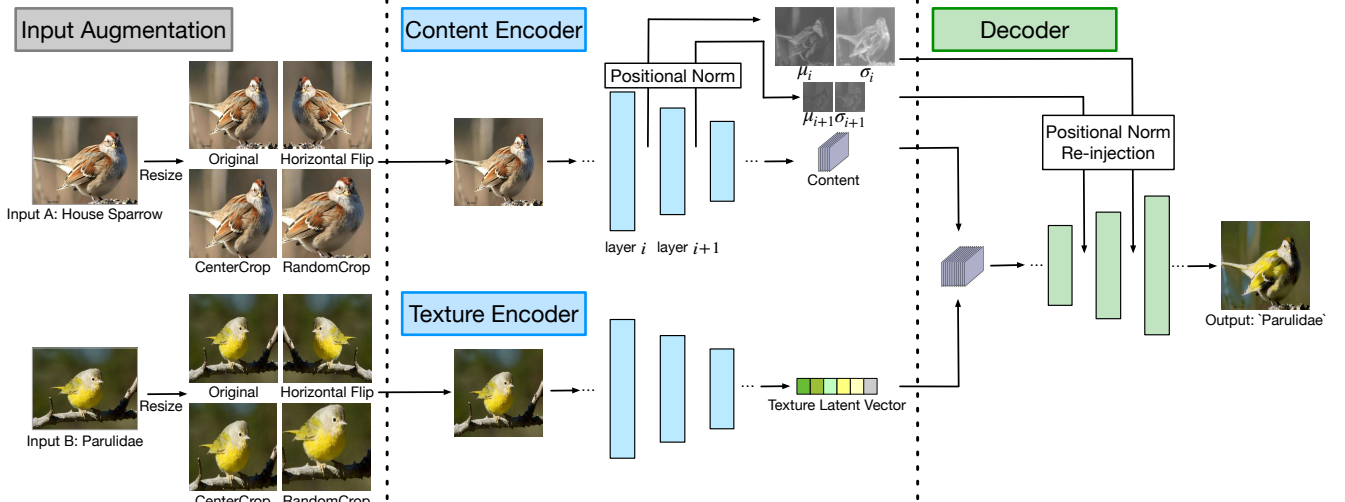


Figure 4. Single Image Texture Translation (SITT) Framework. SITT learns to encode the content and texture from a single content and texture image respectively, then decodes an output image with the texture translated onto the content.

Method	FID ↓	LPIPS ↓	VGG Loss ↓
ArtStyle	237.8	0.682	0.972
CycleGAN	209.6	0.514	0.805
SinGAN	224.5	0.537	0.819
FUNIT	221.8	0.567	0.698
TuiGAN	223.7	0.513	0.791
SITT	197.7	0.509	0.391

Table 1. Quantitative comparison between SITT and several state-of-art image synthesis methods. The lower the better.

we utilize Positional Norm to extract structural information and re-inject them into intermediate layers of decoder. To evaluate the impact of this operation, we compare our results with or without Positional Norm re-injection. In Fig. 6, we show comparisons of similar structural modes and different structural modes that two inputs share similar or different structures. It could be noticed that Positional Norm re-injection effectively regularizes the model to preserve its original content and avoid obvious unclear regions, color distortion and weird spots for a reasonable output.

4.4. Running Time

SITT is a lightweight yet efficient network. Here we show the comparison of average training and testing time per iteration in an epoch using the same single Geforce GTX 1080 Ti GPU without acceleration in Table 2. For testing, we report the time of forward operation. For training, we report the time of forward, backward and optimizer, scheduler update operations. We report the number of training iterations (iters) needed for each method.⁴ For output type, we report

⁴Note: We utilize the official code or the widely used github code. For CycleGAN, we train it for the same number of epochs of SITT to make fair comparisons. For FUNIT, we test the one-shot translation using the official pre-trained model that has been trained for 100,000 iterations, so the

Method	Testing Time ↓	Training Time ↓	Training Iters ↓	Output Type
ArtStyle	0.031	0.036	1000	single
CycleGAN	0.053	0.260	800	pair
SinGAN	0.047	0.099	20000	single
FUNIT	0.080	-	pre-train	pair
TuiGAN	0.051	0.372	20000	pair
SITT	0.009	0.250	800	pair

Table 2. Comparisons of testing time and training time (seconds per iteration) and corresponding training details.

Training data	ResNet-18	VGG16
sick_single	55.2	55.2
sick_repeat	65.7	64.6
sick_aug _{sitt}	70.7	71.3

Table 3. Healthy / sick leaves classification results (Top-1 accuracy %) with different training dataset.

whether the model generates a pair of outputs ('pair') or a single output ('single'). The implementation of various methods are based on Pytorch [32]. We set image size as 288×288 in all code for fair comparison. We could notice that SITT achieves fastest testing with an obvious edge. Though ArtStyle could be trained very fast, it cannot achieve texture translation very well. While SITT shows its superior advantage considering training iterations and training time (seconds/iter) as well as model performance in general.

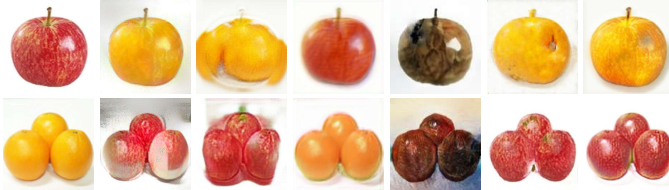
5. SITT for Data Augmentation

In this section we explore SITT for data augmentation and display some promising results on several challenging natural datasets.

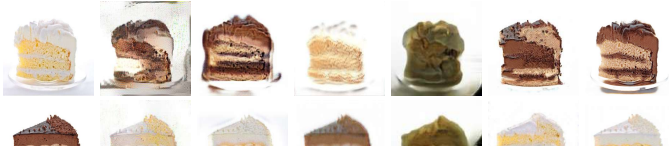
'training time' is '–', 'training iters' is 'pre-train'. We report the training time of SinGAN and TuiGAN at Scale=0, which costs less time than other scales.



(a) Horse \leftrightarrow Zebra.



(b) Apple \leftrightarrow Orange.



(c) VanillaCake \leftrightarrow ChocolateCake.

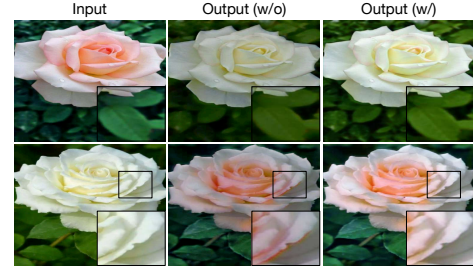


(d) Milk \leftrightarrow BubbleMilk.

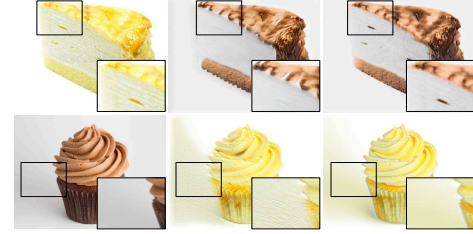
Figure 5. Qualitative comparison between SITT and several state-of-the-art image synthesis methods.

5.1. Long-Tailed Image Classification

In the wild, it is very hard and impractical to collect balanced datasets for training recognition models. For example, collecting healthy leaves is easy, while collecting sick leaves could be comparatively very difficult and expensive. In this section, we use SITT to translate the texture from the few sick leaves to the healthy leaves to obtain more ‘sick’ data. We use Plant Pathology 2020 dataset [41] that provides data covering a number of category of foliar diseases in apple trees. We select ‘healthy’ and ‘multi-disease’ classes as ‘healthy’ and ‘sick’ and randomly split the dataset for training and testing. The training set consists of 416 healthy images and 1 sick image, the test set consists of 100 healthy images and 81 sick images. On the whole, we have three types of training data: sick_single, sick_repeat and sick_aug_{sitt}. We refer to the single sick image as sick_single. We repeat the single sick image to match the ‘healthy’ data count, and refer to this dataset as sick_repeat. Then we apply the texture



(a) Similar structural modes.



(b) Different structural modes.

Figure 6. Comparison w/ or w/o Positional Norm re-injection.



Figure 7. sick_{aug}_{sitt} visualization.

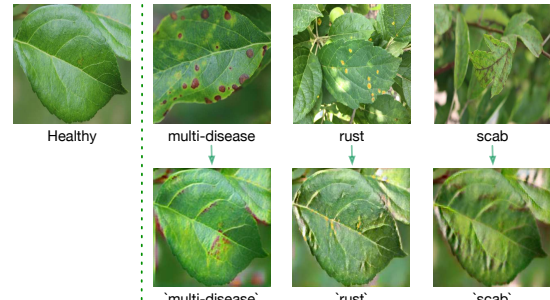


Figure 8. Augmented data (multiple classes) visualization.

from the single sick leaf to all healthy leaves via SITT; we call this augmented set as sick_{aug}_{sitt} (Please see Fig 7 for examples). To validate the augmented sick_{aug}_{sitt}, we use t-SNE [26] to visualize the distribution of sick_{repeat}, targeted test set, and sick_{aug}_{sitt}. In Fig. 9, we see that the augmented data shares a similar t-SNE distribution with the targeted test data. We train and test with these datasets on ResNet-18 [14] and VGG16 [38] using cosine learning rate

Method	2-class	3-class	4-class
Baseline	55.2	8.4	7.8
Repeat	61.9	23.4	28.8
Repeat + Colorjitter	64.6	35.5	35.5
Repeat + GaussianBlur	63.0	23.7	29.6
Repeat + Grayscale	65.2	28.9	32.9
Aug_{sitt}	70.7	27.4	30.7
Aug_{sitt} + Colorjitter	69.6	38.8	36.6
Aug_{sitt} + GaussianBlur	68.5	24.7	30.0
Aug_{sitt} + Grayscale	66.9	34.4	37.0

Table 4. Multi-class leaves classification results (Top-1 accuracy %) with various augmentation strategies based on ResNet-18.

starting from 0.01 for 90 epochs⁵ with standard augmentation RandomResizedCrop and RandomHorizontalFlip. We run experiments for three times and report the average score for fair comparison. In Table 3, we could observe consistent superior results of sick_aug_{sitt} over the baselines.

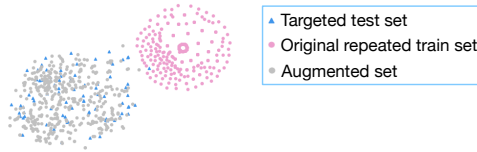


Figure 9. t-SNE visualization with leaf images.

Complementarity with other augmentation methods. SITT is a simple yet efficient method to generate new data semantically, and we may regard it as complimentary with other existing augmentation methods. To justify this, we further explore leaf classification in the multiple classes setting. We add the other classes ‘rust’ and ‘scab’ from Plant Pathology 2020 [41], aiming to classify which category the leaves belong to. We randomly split the dataset for training and testing. The training set consists of 416 healthy leaf images, 1 multi-disease, 1 rust and 1 scab leaf image, the test set consists of 100 healthy, 81 multi-disease, 612 rust and 582 scab leaf images. We take all four categories for 4-class classification and healthy, rust, scab leaf images for 3-class classification, as well as healthy, multi-disease for 2-class classification. Same as previous setting, we treat the original training data as baseline. We call the repeat operation as Repeat and augmentation via SITT as Aug_{sitt} (Please see Fig 8 for augmented examples). Then we combine Repeat and Aug_{sitt} with three popular augmentation methods [4] including Colorjitter, GaussianBlur, and Grayscale. In Table 4, we show the comparison of various augmentation strategies based on ResNet-18. Consistent with previous results, Aug_{sitt} improves the baseline with a large margin. We also note that Aug_{sitt} could be compatible with other augmentation methods and help improve test results.

⁵The model has already converged within 90 epochs. Others follow the original setting.

Method	ResNet-18	VGG16	ResNet-50
Baseline	76.2	77.7	81.8
Aug_{sitt}	77.7	79.2	82.7

Table 5. Comparison of all-way 5-shot classification (Top-1 accuracy %) results on Oxford 102 flowers.

Method	ResNet-18	VGG16	ResNet-50
Baseline	31.1	40.4	38.6
Aug_{sitt}	32.5	40.5	38.9

Table 6. Comparison of all-way 5-shot classification (Top-1 accuracy %) results on CUB-200-2011.

5.2. Few-shot Image Classification

Modern recognition systems are data-intensive and often need many examples of each class to saturate performance. However, it is impractical and hampered when the data set is small. Few-shot learning [48, 47] is proposed to solve such kind of problem and improve the recognition performance by training with few samples. In this section, SITT aims to generate additional training images for improving few-shot image classification. Here we set up all-way few-shot (few images of all classes) classification based on Oxford 102 flowers dataset [29] that consists of 102 flower categories, each class consists of between 40 and 258 images. We strictly follow the official data split rule. For training, we randomly select 5 images as 5 shots for each class, for testing, we evaluate the model on all test images. We augment the data within each category, each image is augmented to 4 additional images based on the new content of other 4 images (Please see Appendix Section D for a bunch of visualization examples), therefore we have 25 images for each class, we call this setting as Aug_{sitt} . To make fair comparison, for baseline, we repeat 5 images of each category for 4 times to ensure the same numbers of train set. Since all-way 5-shot 102 classes classification is very difficult to train from scratch [40], we fine-tune the pre-trained model and test on the official testset based on ResNet-18, VGG16 and ResNet-50 (all of which have been pretrained on the 1000-class ImageNet [6])⁶. We run the experiments for 3 times and report the average score in Table 5. It could be obviously noticed that Aug_{sitt} is able to improve the classification on 102 classes without any additional fine-tuning on real images. The results are very inspiring and show the consistent edge regarding different model architectures.

To further verify the validity of SITT, we strictly follow the same procedure of Oxford flowers setting and apply SITT to Caltech-UCSD Birds-200-2011 (CUB-200-2011) dataset [45] for data augmentation (Please see Appendix Section D for a gallery of visualization examples). CUB-200-2011 consists of 11,788 photos of 200 bird species. We run

⁶For fine-tuning, we fine-tune the Pytorch default pre-trained model for 90 epochs and set cosine learning rate starting from 0.01.

Training data	ResNet-18	VGG16
Baseline	50.0	50.0
Repeat	57.1	63.8
Aug_{sitt}	61.4	68.6

Table 7. Comparisons of Bird Classification (Top-1 accuracy %).

the experiments for 3 times and report the average classification score on the official testset in Table 6. We observe the consistent and competitive improvement of Aug_{sitt} , which sheds light on the feasibility of SITT for few-shot learning tasks.

5.3. SITT for Data Augmentation in the Wild

In this section, we talk about SITT for two applications with natural images in the wild. Beyond these, please see Appendix Section C for more study and results as well as Appendix Section D for more augmented examples on natural images using SITT.

Bird Classification. iNaturalist (iNat) [44] is a large-scale species classification and detection dataset that features visually similar species, captured in a wide variety of situations from all over the world. We select two genera House Sparrow and Parulidae under the Aves (or bird) supercategory from iNat 2018 (training images) that provides data and labels based on biology taxonomy. We randomly split the dataset into train and test. The training set consists of 518 Parulidae images and 1 House Sparrow image, both test set consists of 105 images separately. Since the two categories share similar structures, we are able to use SITT to generate synthetic images with translated textures. Please see Figure 2 for illustration. Following previous long-tailed classification settings, we compare the classification results of Baseline, Repeat and Aug_{sitt} and display them in Table 7. It could be observed that augmented birds are able to help improve the classification performance, which is consistent with the results of leaf classification.

Camouflage. Mimicry or Camouflage in natural world provides some real examples for texture swapping that creatures make the textures of their body similar to the environment’s to avoid danger or hunt food [42]. For instance, we show the case of mantis and orchid. To prey for the insects, mantis will adaptively change their texture similar to the orchids. In Figure 10, we give an illustration and find SITT could translate the orchids’ texture to the mantis and obtain reasonable and natural outputs that looks very close to the real example.

6. Discussion

Task-specific augmentation. In this paper, we introduce task- and dataset-specific augmentation. We aim to swap the texture between a target object (for shape) and an exemplar object (for texture). Therefore, we don’t want the shape with

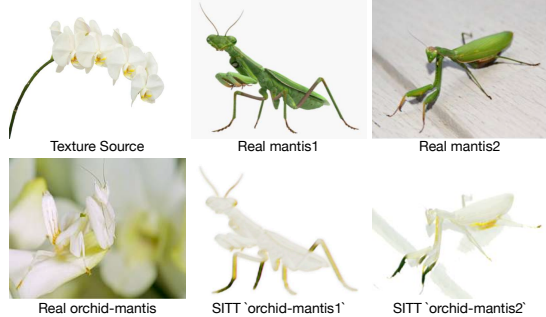


Figure 10. Augmented Orchid-Mantis for camouflage.

the new texture confuses with other classes in the dataset. In traditional image recognition pipelines, image augmentation includes rotation, crop, jittering, flip, etc. Recently, [52, 22] revised input data or features to improve image classification performance. On the one hand, these methods change the way of representation while keeping the texture the same. On the other hand, image synthesis brings a new direction to change the texture while keeping the structure unchanged. Such kind of augmentation engineering opens a door for understanding objects from textures to structure, as well as augmenting data by ‘destroy’ the original textures while replacing them with sensible or other resources.

Label assignments for augmented data. Image synthesis brings a new world for data augmentation. Previous methods mainly focus on leading networks to learn more shape information by applying different styles to the original images [10, 56, 39]. In these cases, the augmented image will be assigned with the original label. However, label assignments should be seriously considered given different tasks and datasets. For leaves classification, the difference between sick and healthy leaves are textures. Therefore, we generate a bunch of sick leaves by translating the textures of sick leaves to healthy leaves and assign the new image as ‘sick’ instead of ‘healthy.’ While for few-shot learning experiments, we augment the data within each category and assign the same label to them. For future potential directions, more advanced label assignment strategies such as label perturbation [52, 51, 22] could be considered for synthetic dataset.

Limitations. Although SITT brings an obvious improved margin for recognition models, sometimes there are very few provided texture source images. Therefore the extracted texture information via SITT might not be able to cover all texture patterns in testset, leading to limited accuracy improvement. Besides, despite of faster running time, there still be a processing time gap between image synthesis and traditional data augmentation such as flip and crop. For the future work, we would explore on both optimally increasing the diversity based on the single or very few texture source and speeding up the image translation model. We believe these signals shed light on the new research direction of

semantic image synthesis for data augmentation.

7. Conclusion

In this paper, we proposed an efficient method (SITT) to translate texture from one image to another. Images generated by SITT not only look appealing but also help visual recognition tasks including long-tailed and few-shot image classification. We hope our work could open the door of using image synthesis for data augmentation in various computer vision tasks and make image synthesis one step closer to solving real problems in the wild.

References

[1] Antreas Antoniou, Amos Storkey, and Harrison Edwards. Data augmentation generative adversarial networks. *arXiv preprint arXiv:1711.04340*, 2017. 2

[2] Tolga Bolukbasi, Kai-Wei Chang, James Y Zou, Venkatesh Saligrama, and Adam T Kalai. Man is to computer programmer as woman is to homemaker? debiasing word embeddings. *Advances in neural information processing systems*, 29:4349–4357, 2016. 2

[3] Ting Chen, Simon Kornblith, Mohammad Norouzi, and Geoffrey Hinton. A simple framework for contrastive learning of visual representations. *arXiv preprint arXiv:2002.05709*, 2020. 2

[4] Xinlei Chen, Haoqi Fan, Ross Girshick, and Kaiming He. Improved baselines with momentum contrastive learning. *arXiv preprint arXiv:2003.04297*, 2020. 2, 7

[5] Ekin D Cubuk, Barret Zoph, Dandelion Mane, Vijay Vasudevan, and Quoc V Le. Autoaugment: Learning augmentation strategies from data. In *Proceedings of the IEEE conference on computer vision and pattern recognition*, pages 113–123, 2019. 2

[6] Jia Deng, Wei Dong, Richard Socher, Li-Jia Li, Kai Li, and Li Fei-Fei. Imagenet: A large-scale hierarchical image database. In *2009 IEEE conference on computer vision and pattern recognition*, pages 248–255. Ieee, 2009. 7

[7] Alexei A Efros and William T Freeman. Image quilting for texture synthesis and transfer. In *Proceedings of the 28th annual conference on Computer graphics and interactive techniques*, pages 341–346, 2001. 1

[8] Leon A Gatys, Alexander S Ecker, and Matthias Bethge. A neural algorithm of artistic style. *arXiv preprint arXiv:1508.06576*, 2015. 4

[9] Leon A Gatys, Alexander S Ecker, and Matthias Bethge. Image style transfer using convolutional neural networks. In *Proceedings of the IEEE conference on computer vision and pattern recognition*, pages 2414–2423, 2016. 1, 2

[10] Robert Geirhos, Patricia Rubisch, Claudio Michaelis, Matthias Bethge, Felix A Wichmann, and Wieland Brendel. Imagenet-trained cnns are biased towards texture; increasing shape bias improves accuracy and robustness. *arXiv preprint arXiv:1811.12231*, 2018. 1, 2, 8

[11] Ian Goodfellow, Jean Pouget-Abadie, Mehdi Mirza, Bing Xu, David Warde-Farley, Sherjil Ozair, Aaron Courville, and Yoshua Bengio. Generative adversarial nets. *Advances in neural information processing systems*, 27:2672–2680, 2014. 2, 3

[12] Kaiming He, Haoqi Fan, Yuxin Wu, Saining Xie, and Ross Girshick. Momentum contrast for unsupervised visual representation learning. In *Proceedings of the IEEE/CVF Conference on Computer Vision and Pattern Recognition*, pages 9729–9738, 2020. 2

[13] Kaiming He, Jian Sun, and Xiaou Tang. Guided image filtering. *IEEE transactions on pattern analysis and machine intelligence*, 35(6):1397–1409, 2012. 1

[14] Kaiming He, Xiangyu Zhang, Shaoqing Ren, and Jian Sun. Deep residual learning for image recognition. In *Proceedings of the IEEE conference on computer vision and pattern recognition*, pages 770–778, 2016. 6

[15] Martin Heusel, Hubert Ramsauer, Thomas Unterthiner, Bernhard Nessler, and Sepp Hochreiter. Gans trained by a two time-scale update rule converge to a local nash equilibrium. *arXiv preprint arXiv:1706.08500*, 2017. 4

[16] Xun Huang, Ming-Yu Liu, Serge Belongie, and Jan Kautz. Multimodal unsupervised image-to-image translation. In *ECCV*, 2018. 4

[17] Phillip Isola, Jun-Yan Zhu, Tinghui Zhou, and Alexei A Efros. Image-to-image translation with conditional adversarial networks. In *Proceedings of the IEEE conference on computer vision and pattern recognition*, pages 1125–1134, 2017. 1

[18] Justin Johnson, Alexandre Alahi, and Li Fei-Fei. Perceptual losses for real-time style transfer and super-resolution. In *European conference on computer vision*, pages 694–711. Springer, 2016. 4

[19] Diederik P Kingma and Max Welling. Auto-encoding variational bayes. *arXiv preprint arXiv:1312.6114*, 2013. 2

[20] Hsin-Ying Lee, Hung-Yu Tseng, Jia-Bin Huang, Maneesh Kumar Singh, and Ming-Hsuan Yang. Diverse image-to-image translation via disentangled representations. In *European Conference on Computer Vision*, 2018. 3, 4

[21] Chloe LeGendre, Wan-Chun Ma, Graham Fyffe, John Flynn, Laurent Charbonnel, Jay Busch, and Paul Debevec. Deeplight: Learning illumination for unconstrained mobile mixed reality. In *Proceedings of the IEEE Conference on Computer Vision and Pattern Recognition*, pages 5918–5928, 2019. 1

[22] Boyi Li, Felix Wu, Ser-Nam Lim, Serge Belongie, and Kilian Q Weinberger. On feature normalization and data augmentation. *arXiv preprint arXiv:2002.11102*, 2020. 2, 8

[23] Boyi Li, Felix Wu, Kilian Q Weinberger, and Serge Belongie. Positional normalization. In *Advances in Neural Information Processing Systems*, pages 1622–1634, 2019. 3

[24] Jianxin Lin, Yingxue Pang, Yingce Xia, Zhibo Chen, and Jiebo Luo. Tuigan: Learning versatile image-to-image translation with two unpaired images. In *European Conference on Computer Vision*, pages 18–35. Springer, 2020. 1, 2, 4

[25] Ming-Yu Liu, Xun Huang, Arun Mallya, Tero Karras, Timo Aila, Jaakko Lehtinen, and Jan Kautz. Few-shot unsupervised image-to-image translation. In *arxiv*, 2019. 2, 4

[26] Laurens van der Maaten and Geoffrey Hinton. Visualizing data using t-sne. *Journal of machine learning research*, 9(Nov):2579–2605, 2008. 2, 6

[27] Ben Mildenhall, Pratul P Srinivasan, Matthew Tancik, Jonathan T Barron, Ravi Ramamoorthi, and Ren Ng. Nerf: Representing scenes as neural radiance fields for view synthesis. *arXiv preprint arXiv:2003.08934*, 2020. 1

[28] Maria-Elena Nilsback and Andrew Zisserman. A visual vocabulary for flower classification. In *IEEE Conference on Computer Vision and Pattern Recognition*, volume 2, pages 1447–1454, 2006. 12

[29] Maria-Elena Nilsback and Andrew Zisserman. Automated flower classification over a large number of classes. In *2008 Sixth Indian Conference on Computer Vision, Graphics & Image Processing*, pages 722–729. IEEE, 2008. 7, 12

[30] Taesung Park, Alexei A. Efros, Richard Zhang, and Jun-Yan Zhu. Contrastive learning for unpaired image-to-image translation. In *European Conference on Computer Vision*, 2020. 2

[31] Taesung Park, Jun-Yan Zhu, Oliver Wang, Jingwan Lu, Eli Shechtman, Alexei Efros, and Richard Zhang. Swapping autoencoder for deep image manipulation. *Advances in Neural Information Processing Systems*, 33, 2020. 1, 2

[32] Adam Paszke, Sam Gross, Francisco Massa, Adam Lerer, James Bradbury, Gregory Chanan, Trevor Killeen, Zeming Lin, Natalia Gimelshein, Luca Antiga, et al. Pytorch: An imperative style, high-performance deep learning library. *arXiv preprint arXiv:1912.01703*, 2019. 4, 5

[33] Zhiwei Qin, Zhao Liu, Ping Zhu, and Yongbo Xue. A gan-based image synthesis method for skin lesion classification. *Computer Methods and Programs in Biomedicine*, 195:105568, 2020. 2

[34] Kanishka Rao, Chris Harris, Alex Irpan, Sergey Levine, Julian Ibarz, and Mohi Khansari. Rl-cyclegan: Reinforcement learning aware simulation-to-real. In *Proceedings of the IEEE/CVF Conference on Computer Vision and Pattern Recognition*, pages 11157–11166, 2020. 2

[35] Tamar Rott Shaham, Tali Dekel, and Tomer Michaeli. Singan: Learning a generative model from a single natural image. In *Proceedings of the IEEE International Conference on Computer Vision*, pages 4570–4580, 2019. 1, 2, 4

[36] Connor Shorten and Taghi M Khoshgoftaar. A survey on image data augmentation for deep learning. *Journal of Big Data*, 6(1):1–48, 2019. 1, 2

[37] Ashish Shrivastava, Tomas Pfister, Oncel Tuzel, Joshua Susskind, Wenda Wang, and Russell Webb. Learning from simulated and unsupervised images through adversarial training. In *Proceedings of the IEEE conference on computer vision and pattern recognition*, pages 2107–2116, 2017. 2

[38] Karen Simonyan and Andrew Zisserman. Very deep convolutional networks for large-scale image recognition. *arXiv preprint arXiv:1409.1556*, 2014. 4, 6

[39] Nathan Somavarapu, Chih-Yao Ma, and Zsolt Kira. Frustratingly simple domain generalization via image stylization. *arXiv preprint arXiv:2006.11207*, 2020. 2, 8

[40] Qianru Sun, Yaoyao Liu, Tat-Seng Chua, and Bernt Schiele. Meta-transfer learning for few-shot learning. In *Proceedings of the IEEE/CVF Conference on Computer Vision and Pattern Recognition (CVPR)*, June 2019. 7

[41] Ranjita Thapa, Noah Snavely, Serge Belongie, and Awais Khan. The plant pathology 2020 challenge dataset to classify foliar disease of apples. *arXiv preprint arXiv:2004.11958*, 2020. 2, 6, 7

[42] Marc Théry and Jérôme Casas. Predator and prey views of spider camouflage. *Nature*, 415(6868):133–133, 2002. 8

[43] Hugo Touvron, Andrea Vedaldi, Matthijs Douze, and Hervé Jégou. Fixing the train-test resolution discrepancy. In *Advances in Neural Information Processing Systems*, pages 8250–8260, 2019. 2

[44] Grant Van Horn, Oisin Mac Aodha, Yang Song, Yin Cui, Chen Sun, Alex Shepard, Hartwig Adam, Pietro Perona, and Serge Belongie. The inaturalist species classification and detection dataset. In *Proceedings of the IEEE conference on computer vision and pattern recognition*, pages 8769–8778, 2018. 8

[45] Catherine Wah, Steve Branson, Peter Welinder, Pietro Perona, and Serge Belongie. The caltech-ucsd birds-200-2011 dataset. 2011. 7

[46] Yulin Wang, Xuran Pan, Shiji Song, Hong Zhang, Gao Huang, and Cheng Wu. Implicit semantic data augmentation for deep networks. In *Advances in Neural Information Processing Systems*, pages 12635–12644, 2019. 2

[47] Yaqing Wang, Quanming Yao, James T Kwok, and Lionel M Ni. Generalizing from a few examples: A survey on few-shot learning. *ACM Computing Surveys (CSUR)*, 53(3):1–34, 2020. 7

[48] Yu-Xiong Wang, Ross Girshick, Martial Hebert, and Bharath Hariharan. Low-shot learning from imaginary data. In *Proceedings of the IEEE conference on computer vision and pattern recognition*, pages 7278–7286, 2018. 7

[49] Tete Xiao, Xiaolong Wang, Alexei A Efros, and Trevor Darrell. What should not be contrastive in contrastive learning. In *International Conference on Learning Representations*, 2021. 2

[50] Jaejun Yoo, Youngjung Uh, Sanghyuk Chun, Byeongkyu Kang, and Jung-Woo Ha. Photorealistic style transfer via wavelet transforms. In *International Conference on Computer Vision (ICCV)*, 2019. 2

[51] Sangdoo Yun, Dongyoon Han, Seong Joon Oh, Sanghyuk Chun, Junsuk Choe, and Youngjoon Yoo. Cutmix: Regularization strategy to train strong classifiers with localizable features. In *Proceedings of the IEEE International Conference on Computer Vision*, pages 6023–6032, 2019. 2, 8

[52] Hongyi Zhang, Moustapha Cisse, Yann N Dauphin, and David Lopez-Paz. mixup: Beyond empirical risk minimization. *arXiv preprint arXiv:1710.09412*, 2017. 2, 8

[53] Richard Zhang, Phillip Isola, and Alexei A Efros. Colorful image colorization. In *European conference on computer vision*, pages 649–666. Springer, 2016. 2

[54] Richard Zhang, Phillip Isola, Alexei A Efros, Eli Shechtman, and Oliver Wang. The unreasonable effectiveness of deep features as a perceptual metric. In *CVPR*, 2018. 4

[55] Yexun Zhang, Ya Zhang, Qinwei Xu, and Ruipeng Zhang. Learning robust shape-based features for domain generalization. *IEEE Access*, 8:63748–63756, 2020. 2

[56] Xu Zheng, Tejo Chalasani, Koustav Ghosal, Sebastian Lutz, and Aljosa Smolic. Stada: Style transfer as data augmentation. *arXiv preprint arXiv:1909.01056*, 2019. 2, 8

[57] Jun-Yan Zhu, Taesung Park, Phillip Isola, and Alexei A Efros. Unpaired image-to-image translation using cycle-consistent adversarial networks. In *Computer Vision (ICCV), 2017 IEEE International Conference on*, 2017. [1](#), [2](#), [4](#)

A. SITT Workflow

SITT consists of three parts: shared Texture Encoder (En_T), shared Content Encoder (En_C) and corresponding Decoder De_A , De_B for each category. We first feed the Input B I_B into En_T to get texture latent vector T_B and feed texture source Input A I_A into the En_C to get content matrix C_A . Then we feed T_B and C_A into De_B to get I'_B . Translating B's texture to A follows the same procedure. To better preserve the structural information and optimize training, we apply Positional Norm in En_C to extract intermediate normalization constants mean μ as β and standard deviation σ as γ and re-inject them into the later layers of Decoder to transfer structural information. Please see Algorithm 1 for details.

Algorithm 1: SITT Workflow

Result: Translated output I'_A, I'_B
Input: I_A, I_B ;
 initialize En_C, En_T, De_B ;
while not converged **do**
 | Step1: $T_B \leftarrow En_T(I_B)$;
 | $T_A \leftarrow En_T(I_A)$;
 | Step2: $C_A, \beta_A, \gamma_A \leftarrow En_C(I_B)$;
 | $C_B, \beta_B, \gamma_B \leftarrow En_C(I_B)$;
 | Step3: $I'_B \leftarrow De_B(T_B, C_A, \beta_A, \gamma_A)$;
 | $I'_A \leftarrow De_A(T_A, C_B, \beta_B, \gamma_B)$;
 | Step4: Backpropagation;
end

B. Data Augmentation Workflow with SITT

Assume we have plenty of content source images $SetA$ but a few target texture source images $SetB$, the only difference between $SetA$ and $SetB$ is that they contain different textures. Our goal is to synthesize extra ‘B’ data by replacing textures of $SetA$ with the new textures from $SetB$, we call the augmented dataset as $AugSetB$. Please see Algorithm 2 for details.

C. SITT for Data Augmentation in the Wild

Besides Oxford 102 Category flower dataset [29], we also conduct study on 17 Category flower dataset [28] that is composed of 17 category with 80 images for each class. The dataset has been randomly split into 3 different training, validation and test sets. We strictly follow the data split rule. Same with previous all-way 5-shot experimental setting, we randomly select 5 images in each category for training and test the model on the official testset. Based on 3 different split dataset, we run the experiments for 3 times and report the average score of three testsets in Table 8. We could

Algorithm 2: Data Augmentation Workflow (via SITT)

Result: Augmented dataset $AugSetB$
Input: $SetA, SetB$;
if Single to Single **then**
while Image I_A in $SetA$ **do**
 | **while** Image I_B in $SetB$ **do**
 | | initialize SITT;
 | | **while** not converged **do**
 | | | train SITT;
 | | **end**
 | | $I'_B \leftarrow SITT(I_B, I_A)$;
 | | $AugSetB \leftarrow AugSetB \cup I'_B$;
 | **end**
end
else if Single to Multi **then**
while Image I_B in $SetB$ **do**
 | initialize SITT;
 | **while** Image I_A in $SetA$ **do**
 | | **while** not converged **do**
 | | | train SITT;
 | | **end**
 | **end**
 | **while** Image I_A in $SetA$ **do**
 | | $I'_B \leftarrow SITT(I_A, I_B)$;
 | | $AugSetB \leftarrow AugSetB \cup I'_B$;
 | **end**
end

Method	ResNet-18	VGG16	ResNet-50
Baseline	82.1	82.5	84.9
Aug_{sitt}	83.6	83.0	85.1

Table 8. Comparison of all-way 5-shot classification (Top-1 accuracy %) results on Oxford 17 flowers.

observe that the augmented dataset via SITT still brings consistent competitive improvement.

D. More SITT Examples on Natural Images

D.1. Oxford 102 flowers

Please see Figure 11 for details.

D.2. Caltech-UCSD Birds 200

Please see Figure 12 for details.



Figure 11. Augmented Oxford flowers visualization via SITT.

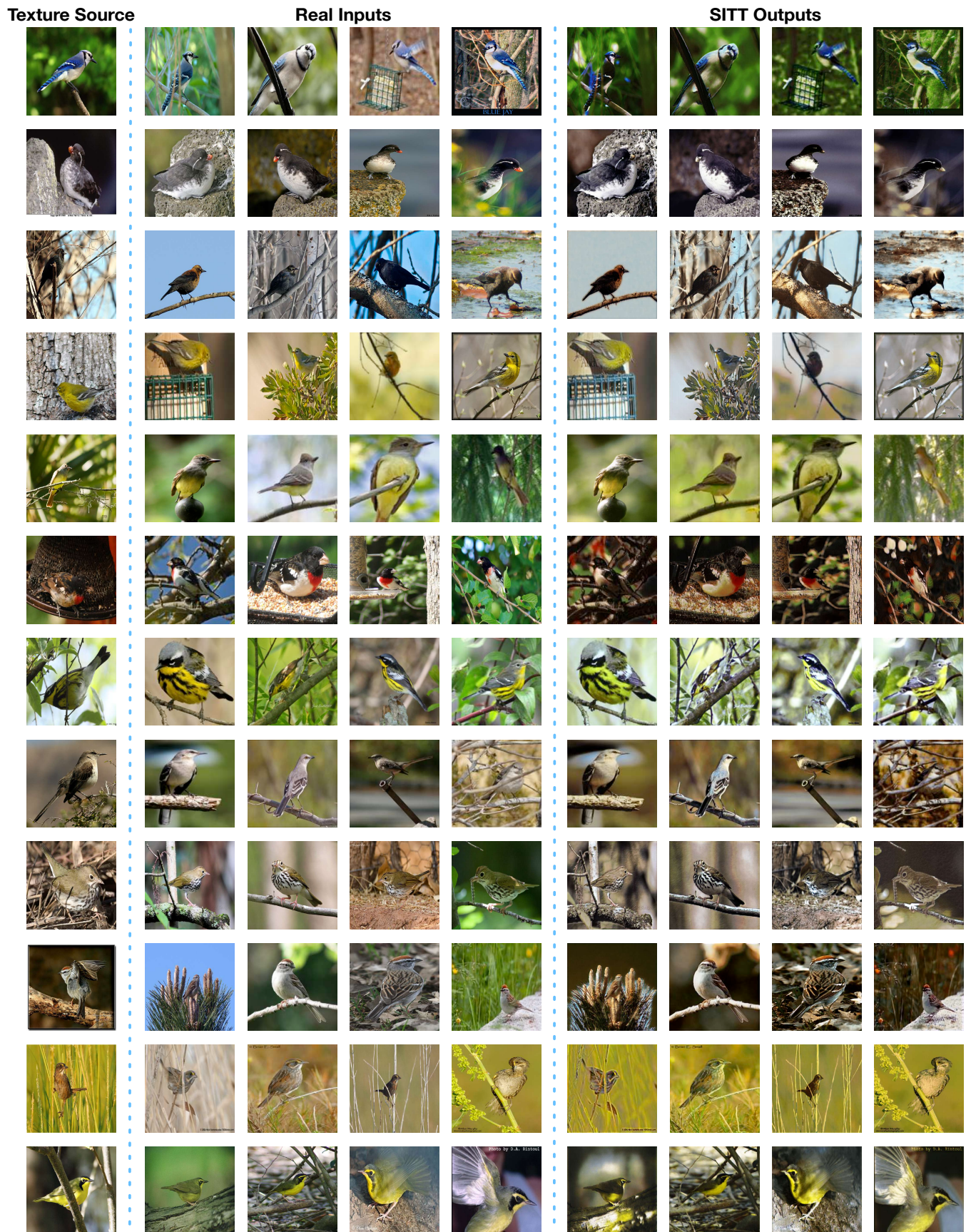


Figure 12. Augmented CUB-200-2011 visualization via SITT.